Further Studies on a Transient Cumulus Cloud Ensemble and Its Large-Scale Interaction

KLAUS FRAEDRICH

Institut für Meteorologie, Freie Universität Berlin, 1 Berlin 33, Germany

(Manuscript received 2 April 1976, in revised form 27 September 1976)

ABSTRACT

A parametric model of a transient cumulus cloud with the related cloud population is introduced. A closure condition is presented which couples the statistical, physical and geometrical parameters of the cloud ensemble with the large-scale circulation. The large-scale sources of latent and sensible heat, as well as the vorticity due to the convective activity of the transient cloud ensemble, can be deduced either with the aid of direct cloud observations or by using the closure condition. The latter approach is applied to undisturbed ATEX 1969 data.

1. Introduction

Three steps are considered for a theory which parameterizes cumulus convection: 1) the development of a sufficiently simple but realistic model of an individual cloud; 2) the construction of an ensemble of these cloud elements; 3) the closure condition which combines the cloud ensemble with the large-scale model.

The above-mentioned three steps are discussed here. The basis is an individual transient cloud and the related cloud ensemble (Fraedrich, 1976) with two kinds of cloud elements, precipitating and nonprecipitating. The cloud ensemble introduced partly follows its own laws, in a statistical sense, by allowing for prescribed but random fluctuations within a large-scale forcing field. The closure condition prescribes this large-scale frame to calibrate the random fluctuations; however, it does not allow a strong coupling between the cloud ensemble and the large-scale processes in a deterministic sense. Section 2 gives the background from an earlier paper (Fraedrich, 1976). The thermodynamic and dynamic budgets of the cloud ensemble, namely, the large-scale sources of sensible and latent heat and vorticity, are derived (Section 3a). Additionally, a parametric method to determine the radiative heating rates due to the existence of a cloud ensemble is described (Section 3b). The closure conditions, presented in Section 4, are used to calculate the source terms due to the convective activity of an undisturbed trade wind situation (Section 5).

2. The mass budget

The budget of the conserved quantity I of a one-dimensional (i.e., area-integrated) cloud is described by a horizontal entrainment (detrainment) process, a divergence of the vertical flux, and time changes (storage) which are related to a horizontal area expansion. This budget is given by[1]

$$\frac{\partial \rho I a}{\partial t}+\frac{\partial m I}{\partial z}=\rho_R I_R \frac{\partial a}{\partial t}-\int_0^a \nabla_h\cdot\rho \mathbf{V} I df, \qquad (2.1)$$

where it has been assumed that the vertical mass flux at the lateral boundary of the cloud vanishes and a top-hat profile has been introduced for the area-averaged cloud properties I, m. In considering I budgets, density fluctuations and horizontal density differences can be neglected. Thus, the mass budget ($I=1$) yields a balance between vertical and horizontal mass flux divergences as given by the anelastic approximation of the continuity equation, i.e., the density is a function of z only.

A simplified mass budget of a transient cloud is obtained after averaging (2.1) over the half-lifetime τ of the cloud life cycle, where the half-lifetime defines the length of the growing or decay period of the cloud process. Assuming the time-averaged cloud mass flux to be vertically constant and the density a function of z only, one obtains

$$0=-\frac{1}{\tau}\int_0^\tau\int_0^a \nabla_h\cdot\rho \mathbf{V} df dt=\rho\oint \tilde{v}_n dl, \qquad (2.2a)$$

with the wind component v_n normal to the lateral boundary of the horizontal cloud area (outflow positive). The tilde indicates the half-lifetime average. The time correlation between normal wind v_n and the boundary length l can be interpreted by the sum of turbulent

[1] A list of symbols is given in an appendix.

fluctuations and a mean motion process. The turbulent fluctuations occur on a smaller time scale than the cloud process averaged with respect to the cloud half-lifetime, i.e.,

$$0=\rho\left\{\oint v'\widetilde{dl'}+\oint\widetilde{v}\,\widetilde{dl}\right\}. \tag{2.2b}$$

The growing period is characterized by turbulent fluctuations deforming the lateral boundary, incorporating environmental air into the cloud process (first term). This is the well-known entrainment mechanism, which is usually assumed to be proportional to the vertical cloud mass flux m_c, where the constant of proportionality is defined as the entrainment factor λ^*. The kinetic energy of these fluctuations is supplied by the buoyancy of the rising thermals which lends further support to the above entrainment parameterization. As a result of this lateral entrainment process the cloud area expands horizontally until it attains its maximum area a_c after the half-lifetime τ (growing period). Thus the cloud-scale divergence [second term of (2.2b)] is interpreted as it is observed, namely, by a cloud area growth due to small-scale entrainment processes at the boundary. The decay phase starts after the cloud has obtained its maximum area. It is characterized by an erosion of the cloud substance into the environment until the cloud area vanishes (lateral detrainment). This turbulent erosion process is accomplished by the environmental wind field because the cloud process is no longer active.

After introducing the above parameterizations of the small- and cloud-scale processes into (2.2b) the mass budget yields

$$\lambda^* m_c=\rho\frac{a_c}{\tau}, \tag{2.3}$$

where the lateral turbulent entrainment process (left-hand side) is realized by an area expansion of the transient cloud (right-hand side). This is in contrast to the entraining jet model where the entrainment process leads to a vertically increasing cloud mass flux. Observations show that large clouds have a long lifetime and vice versa, corroborating the above relationship to be constant. The entrainment factor λ^* is related to the cloud radius r by the empirically determined formula

$$\lambda^*=\frac{3\alpha}{r}. \tag{2.4}$$

TABLE 1. Cloud structure parameters.

	Area expansion (erosion) rate	Depth-width ratio
Disturbed	$c_1\sim10^5$ kg m^{-1} s^{-1}	$\gamma_1\approx0.2$
Undisturbed	$c_2\sim10^4$ kg m^{-1} s^{-1}	$\gamma_2\approx0.5$

Finally, a linear relationship between cloud radius r and cloud depth z_t is suggested by observations and models leading to a width-depth ratio γ:

$$\gamma=\frac{r}{z_t} \tag{2.5}$$

from which the layer depth is determined. Within this layer the cloud mass flux m_c of the individual, time-averaged (transient) cloud can be determined, given its radius or entrainment factor.

Phenomenologically, the relationships (2.3), (2.4) and (2.5) can be summarized such that a large cloud mass flux is related to a small entrainment factor and consequently to a deep, large and long-lasting cumulus cloud and vice versa. [The transient cloud process may also be interpreted from the Lagrangian point of view in terms of a parcel rising from cloud base on top. During the ascent, which takes the half lifetime (the growing period), the parcel entrains environmental properties and detrains cloud properties at the same rate thus keeping the cloud mass flux m_c vertically constant. After the parcel has reached its final depth, or the cloud has reached the state of maturity, the visible cloud, i.e., the stored or detrained cloud substance is laterally mixed into the large-scale environment. Additionally, at the cloud-top final detrainment $m_c\,\delta z^{-1}$ occurs in an infinitesimally thin layer δz.]

Some further, albeit qualitative comments are necessary on the dynamic structure of the individual cumulus cloud as it is characterized by the geometrical parameters c, γ of Eqs. (2.3) and (2.5) and eventually 3α in (2.4). The magnitudes of these constants, describing the (dissipative) structure of cumuli, depend upon the entropy flow through the cloud volume. Thus, a difference between these constants is to be expected for the nonprecipitating and precipating clouds (Table 1). This has been confirmed for the depth-width ratio γ, but observations of the cloud expansion rate (entrainment) c for nonraining clouds is lacking. This structural difference between precipitating and nonprecipitating clouds depends on the large-scale situation (disturbed or undisturbed), the characteristics of which are defined by the closure condition to be discussed in Section 4. However, within a given structure (large-scale situation), the cloud population and its statistics are governed by random processes where the structure parameters c, γ, 3α remain constant.

It can be conjectured that the depth-width ratio of an individual cloud is dependent on the atmospheric stratification of its environment and is thus a function of space and time. Although undoubtedly true, this leads to comprehensive calculations of cloud heights where the correct definition of a cloud top may provide additional problems. However, this geometrical depth-width ratio γ should be interpreted in a statistical sense as a parameter representative for (disturbed or

undisturbed) cloud ensembles which influence or even produce their own environmental stratifications.

Within a large-scale unit area F the ensemble of individual cumulus clouds can be described by an exponential cloud parcel radius distribution function similar to the Marshall-Palmer distribution for rain droplets. The number density is

$$n(r)=K\exp(-\beta r), \tag{2.6}$$

where the coefficients K, β can simply be derived from the total number N_0 and area cover $A_0=\sigma F$ of clouds (σ the relative cloud cover). It is assumed that the profile of the radius distribution function (2.6) is governed by independent random processes. Only the coefficients K, β are controlled by the large-scale fields. Using an infinitely large radius spectrum and circular clouds ($a=\pi r^2$) one obtains the directly observable cloud population parameters

$$N_0=K\beta^{-1}, \quad A_0=2\pi K\beta^{-3}, \tag{2.7}$$

which replace the coefficients K, β of the distribution function (2.6).

The quotient

$$\frac{A_0}{N_0}=\pi R_0^2=2\pi\beta^2$$

gives the average cloud area which is related to a cloud radius R_0 and a characteristic cloud layer depth Z [see (2.5)] of the form

$$Z=\gamma^{-1}R_0=\frac{\sqrt{2}}{\beta\gamma}=\gamma^{-1}\left(\frac{1}{\pi}\frac{A_0}{N_0}\right)^{\frac{1}{2}}=\sqrt{2}\hat{Z} \tag{2.8}$$

which differs from the average cloud-depth $\hat{Z}$ by the factor $\sqrt{2}$, where

$$\hat{Z}=\frac{1}{N_0}\int_0^\infty zK\exp(-\beta r)dr=\frac{1}{\beta\gamma}. \tag{2.9}$$

The formulas (2.7) and (2.9) are not as simple if the radius spectrum is finite.

The mass budget of a transient cumulus cloud ensemble and its vertical variation can now be deduced by integration of the individual cloud mass flux over the radius spectrum using Eqs. (2.3)–(2.6) (see Fraedrich, 1976). Thus, making use of (2.9), the mass flux M_c and its vertical divergence, namely, the final detrainment D_f yields

$$M_c=M_0(z\hat{Z}^{-1}+1)\exp(-z\hat{Z}^{-1}), \tag{2.10a}$$

$$D_f=M_0z\hat{Z}^{-2}\exp(-z\hat{Z}^{-1}), \tag{2.10b}$$

where the cloud mass flux M_0 at cloud base ($z=0$) is

$$M_0=\frac{c}{3\alpha}\left(\frac{N_0A_0}{2\pi}\right)^{\frac{1}{2}}=\frac{c}{3\alpha}\frac{K}{\beta^2}. \tag{2.11}$$

In addition, the lateral area expansion during the growing phase of the cloud life cycle leads to lateral detrainment D_l (erosion) of the cloud ensemble in the decaying phase i.e.,

$$D_l=M_0\hat{Z}^{-1}\frac{3\alpha}{\gamma}\exp(-z\hat{Z}^{-1}). \tag{2.12}$$

Thus the lateral detrainment gives a measure of the recycling rate of air mass by the cloud ensemble. The total mass budget of the transient cumulus cloud ensemble, as given by the vertical mass flux and the final and lateral detrainment, can now be determined from direct cloud observations, the total cloud number N_0 and area A_0. On the other hand, the mass budget can also be calculated if the cloud mass flux M_0 at cloud base and the characteristic cloud depth Z are prescribed by the large-scale parameters of a numerical model. This leads to a closure condition which is discussed in Section 4. Also, it should be mentioned that the mass budget of the cloud ensemble and its vertical distribution do not depend on the structure parameter c (the cloud area expansion rate) if M_0 and Z are known.

3. The large-scale sources

a. Dynamic and thermodynamic sources

In the large-scale budget equations of a conserved quantity there appears a source term Q_I which is due to the convective activity:

$$Q_IF=M_c\frac{\partial\bar{I}}{\partial z}+D_f(I_f-\bar{I})+D_e(I_l-\bar{I}). \tag{3.1}$$

The components of Q_I are compensating subsidence, final detrainment and lateral detrainment of the cloud ensemble; the related properties of the latter two (I_f, I_l) are different and defined below.

For an individual transient cloud, the vertical distribution of the property I_c is given by the well-known entrainment equation (Fraedrich, 1976)

$$\frac{\partial I_c}{\partial z}=\lambda^*(\bar{I}-I_c). \tag{3.2}$$

For simplicity a linear large-scale distribution $I_0+\Gamma_Iz$ is introduced. One obtains for the difference between cloud and environmental property

$$\Delta I(\lambda^*,z)=I_c-\bar{I}=\Delta I_0\exp(-\lambda^*z)-\Gamma_I/\lambda^*[1-\exp(-\lambda^*Z)]. \tag{3.3}$$

Lateral and final detrainment of an individual cloud are given by

$$d_l\Delta I_l=\lambda^*m_c\Delta I(\lambda^*,z); \quad d_f\Delta I_f=m_c\delta z^{-1}\Delta I(\lambda^*,z=z_t), \tag{3.4}$$

where the lateral detrainment $d_l=\lambda^*m_c$ occurs between cloud base and top ($z=z_t$), and the final detrainment at

the cloud top within an infinitesimally thin layer δz. After making some algebraic transformations, integration over the cloud ensemble yields the vertical distribution of the lateral detrainment

$$\left.\begin{aligned} D_l(I_l-\bar{I}) &= \int_0^{\lambda^*(z_t)} \Delta I(\lambda^*,z)\,dD_l \\ dD_l &= M_0\left(\frac{3\alpha}{\gamma\hat{Z}\lambda^*}\right)^2 \exp\left(-\frac{3\alpha}{\gamma\hat{Z}\lambda^*}\right)d\lambda^* \end{aligned}\right\}. \quad (3.5)$$

All clouds of the ensemble contribute to the lateral detrainment. The final detrainment of the cloud ensemble is independent of the entrainment factor as it occurs at the cloud top $z=z_t=3\alpha/(\gamma\lambda^*)$ [see Eq. (3.5)]. Only clouds with their tops reaching this height contribute to the final detrainment of the ensemble, i.e.,

$$D_f(I_f-\bar{I}) = D_f\left[\Delta I_0 \exp\left(-\frac{3\alpha}{\gamma}\right) - \Gamma_I\left(\frac{\gamma z}{3\alpha}\right)\left(1-\exp\left(-\frac{3\alpha}{\gamma}\right)\right)\right]. \quad (3.6)$$

The large-scale sources Q_I can now be calculated, given the large-scale distribution of the property $\bar{I}$, the condition at cloud base I_{c0} and from the closure condition (or from direct observations of cloud cover and number) the cloud-base mass flux M_0 with the characteristic cloud-layer depth $Z=\hat{Z}(2)^{\frac{1}{2}}$.

The apparent sources Q_I due to cumulus clouds satisfy the constraint

$$\int_0^\infty Q_I dz = M_0 F^{-1}\Delta I_0. \quad (3.7)$$

Considering separately, the vertically integrated processes of the so-called compensating subsidence, final and lateral detrainment [Eq. (3.1)] one obtains

$$\int_0^\infty M_c F^{-1}\frac{\partial \bar{I}}{\partial z}dz = M_0 F^{-1} 2\Gamma_I \hat{Z}, \quad (3.8)$$

$$\int_0^\infty D_f F^{-1}(I_f-\bar{I})dz = M_0 F^{-1}\left\{\Delta I_0 \exp\left(-\frac{3\alpha}{\gamma}\right) - 2\Gamma_I\hat{Z}\frac{\gamma}{3\alpha}\left[1-\exp\left(-\frac{3\alpha}{\gamma}\right)\right]\right\}, \quad (3.9)$$

$$\int_0^\infty D_l F^{-1}(I_l-\bar{I})dz = M_0 F^{-1}\left\{\left(\Delta I_0+2\Gamma_I\hat{Z}\frac{\gamma}{3\alpha}\right) \times\left[1-\exp\left(-\frac{3\alpha}{\gamma}\right)\right]-2\Gamma_I\hat{Z}\right\}. \quad (3.10)$$

The sum of (3.8)–(3.10) fulfills the constraint (3.7) as requested.

b. Radiative flux divergences

In the following an attempt is made to describe how the radiative heating rates due to the convective activity may be considered as additional terms of the convective heat sources (3.1). These radiative heating rates will be separated into a longwave emission from and shortwave absorption within the cumulus cloud ensemble.

1) SHORTWAVE RADIATIVE HEATING

A simple first-order estimate of the shortwave absorption within a one-dimensional transient cumulus cloud (and the related ensemble) is based on the assumptions that (i) it is uniformly distributed in the vertical cloud column, (ii) it is proportional to the mass-averaged total specific water content ($x=q+l$):

$$P=\int_0^{z_t} x\rho dz \Big/ \int_0^{z_t}\rho dz.$$

and (iii) it is proportional to the global (direct+diffusive) shortwave flux density G.

This leads to the shortwave heating rate of an individual cloud

$$k=\epsilon_k GP$$

and of the cloud ensemble after integration over the total cloud area,

$$K=\int_r^\infty k\pi r'^2 n(r')dr'. \quad (3.11)$$

The vertical variation is obtained by introducing the height-radius ratio (2.5). The term $\epsilon_k\sim 10^{-2}$ m^{-2} is a constant of proportionality and has been determined by numerical and observational radiative experiments (Grassl, personal communication).

The large-scale heating by shortwave processes due to the convective activity of the transient cloud ensemble is identical to (3.11), because the radiative processes affect those properties laterally detrained from the rising cloud parcels during the growing period which form the visible cloud. At the end of the cloud life cycle (decay phase) the locally stored (detrained) cloud properties of the visible cloud are laterally mixed into the environment where the radiative effects have been included.

2) LONGWAVE RADIATIVE COOLING

The first-order estimate of the longwave emission e from the individual transient cloud is based on the assumptions (i) that it occurs only at the cloud top z_t where it is proportional to (ii) the total water content $x(z_t)$, and (iii) that the blackbody emission σT^4 may be

written

$$e=\epsilon_e x(z_t)\sigma T_t^4.$$

Here $\epsilon_e \sim 10^{-1}$ m^{-1} is the constant of proportionality (Grassl, personal communication).

The total water content $x(z_t)$ at the cloud top is obtained by (3.3) [for $I=x$, with $\lambda^*=3\alpha/(\gamma z)$ and $z=z_t$]. The temperature representing the blackbody emission may be prescribed by the large-scale temperature at cloud top (z_t) because at this height cloud parcels are assumed to be close to equilibrium with the environment, i.e., without buoyancy.

Thus after integration over the cloud area the longwave emission from the cloud ensemble may be written

$$E=e\left[\frac{1}{F}\int_r^\infty \pi r'^2 n(r')dr'\right], \tag{3.12}$$

where factor in brackets is the vertical distribution of the fractional cloud cover; after some algebraic transformations, using (2.5), (2.7), (2.11), this may be written

$$A_0F^{-1}\left(1+\frac{z}{\hat{Z}}+2\frac{z^2}{\hat{Z}^2}\right)\exp(-z\hat{Z}^{-1}).$$

The large-scale radiative cooling rate due to the presence of transient clouds is identical to (3.12). Arguments similar to those for shortwave radiation hold for longwave processes, because those cloud properties being affected by longwave emission are mixed into the environment due to the final detrainment process at the cloud top. Some calculations of the large-scale radiative heat sources as parameterized above are described at the end of Section 5.

4. Closure conditions

Two closure conditions are necessary to determine the magnitude of the number density function (2.6) which characterizes all properties of the transient cloud ensemble. Therefore, the coefficients K and β must be prescribed, for example, by an observational closure using the directly observable cloud population parameters A_0, N_0 and Eq. (2.7); or K and β can be deduced from (2.9) and (2.11) if the characteristic cloud-layer depth Z and the ensemble mass flux M_0F^{-1} at cloud base are known. Some suggestions for such a physical closure condition are discussed in the following.

The statistical properties of the cloud ensemble are characterized by the cloud-layer depth Z where the random behavior (prescribed by the exponential number-density distribution) of the cloud elements is determined by large-scale constraints: an insufficient heat (or entropy) flow through a large-scale unit volume keeps the internal (dissipative) structure of the cloud elements low (nonprecipitating clouds). Beyond a given threshold (i.e., for a specific magnitude of large-scale convergence) the cloud structure changes toward a higher order (precipitating clouds), but the random distribution function is assumed to remain the same (see Table 1).

Therefore, it appears appropriate to relate the parameters of the closure conditions (M_0F^{-1}, Z) to properties which characterize a large-scale unit volume with respect to the convective activity within it. As the convective processes are directly connected with the surface fluxes (which needs not necessarily be the case for stratiform clouds), this unit volume may be divided into a lower and upper part by the level where the large-scale horizontal divergence (e.g., of total energy) changes its sign. This height is assumed to be identical to the characteristic cloud-layer depth Z above cloud base z_0, i.e.,

$$0=\nabla\cdot\overline{\rho\mathbf{V}}\,|_{z+z_0}. \tag{4.1}$$

Another fundamental parameter is the large-scale mass (or energy) recycling rate

$$\bar{\delta}=\int_0^F\int_{z_0}^{Z+z_0}|\nabla\cdot\rho\mathbf{V}|\,dz\,df\approx F\,|\overline{\rho w}|_{z+z_0}, \tag{4.2}$$

which is measured by the total mass flow through the large-scale unit volume. The life cycle of the clouds determines the (mass) recycling rate δ_c of air by the cumulus ensemble embedded in the large-scale unit volume:

$$\delta_c=F^{-1}\int_{z_0}^{Z+z_0}D_l dz=M_0F^{-1}\frac{3\alpha}{\gamma}[1-\exp(-Z\hat{Z}^{-1})]. \tag{4.3}$$

The convective activity is assumed to adjust itself to the large-scale processes (mass flux) in such a way that all the air within the large-scale unit volume can be modified (only) once by the cloud ensemble before it is exchanged, i.e., the most efficient modification of a large-scale ventilation. This leads to an equilibrium between cloud ensemble and the large scale which is defined by the same recycling rates $\bar{\delta}=\delta_c$, leading to the second closure ($Z\hat{Z}^{-1}=\sqrt{2}$):

$$M_0F^{-1}\frac{3\alpha}{\gamma}[1-\exp(-Z\hat{Z}^{-1})]=|\overline{\rho w}|_{z+z_0}. \tag{4.4}$$

Instead of (4.4) a closure condition similar to Kuo's (1974) may be introduced where the (steady-state) moisture budget of the large-scale unit volume is balanced by the water budget of the cloud ensemble. However, the deficiency of no large-scale storage must be faced by any such budget closure (e.g., Cho, 1976).

The combination of (4.1) and (4.4) with (2.8), (2.9) and (2.11) gives the area cover and the number of the transient cumulus clouds. Incorporating the above closure conditions one obtains

$$N_0=\left(\sqrt{2}\frac{3\alpha}{\gamma}\right)\frac{M_0}{Z};\quad A_0=\left(\pi\sqrt{2}\frac{3\alpha}{c}\gamma\right)ZM_0. \tag{4.5}$$

TABLE 2. Boundary conditions for the cloud ensemble budgets (ATEX, February 1969).

$M_0F^{-1}=3\times10^{-2}$ kg m^{-2} s^{-1}	
$Z=10^3$ m	
$\Delta S_{w0}=0$	$\Gamma_s=+3$ J kg^{-1} m^{-1}
$\Delta(q+l)_0=5\times10^3$ J kg^{-1}	$\Gamma_q=-8$ J kg^{-1} m^{-1}
$\Delta h_0=5\times10^3$ J kg^{-1}	$\Gamma_h=-5$ J kg^{-1} m^{-1}
$\Delta W_0=0$	$\Gamma_w=\Gamma_h\Gamma_\xi\rho^{-1}$
$\bar{\xi}_0=-5\times10^{-6}$ s^{-1}	$\Gamma_\xi=-1\times5\ 10^{-6}$ s^{-1} 10^{-3} m^{-1}

The closure conditions may be summarized as follows: the vertical extent of the large-scale convergent or divergent flux dictates the characteristic cloud-layer depth Z; the horizontal extension of the large-scale fluxes defines the spread of the cloud ensemble; its sign (convergent or divergent) denotes the internal structure of the cloud elements; and the mass (or energy) recycling of the large-scale volume determines the recycling rate of the cloud ensemble due to the life cycle of the cumuli. Thus, the closure conditions and the structure coefficients (Table 1) describe the combined statistical and structural behavior of the cloud ensemble where the transient cumulus cloud structure is mainly characterized by its geometrical appearance. The thermodynamic and dynamic boundary conditions necessary for a calculation of the physical cloud ensemble properties can be provided by a subcloud-layer model and the large-scale environment; this is not discussed here.

5. Application to ATEX undisturbed period: 7–12 February 1969

The moist static energy h, the liquid water static energy S_w and total water content x are thermodynamic quantities individually conserved for isobaric mixing (Betts, 1975), i.e.,

$$\left.\begin{aligned} h&=c_pT+gz+Lq\\ S_w&=c_pT+gz-Ll\\ x&=q+l \end{aligned}\right\}. \tag{5.1a}$$

The vertical component of Ertel's circulation constant W (pseudopotential vorticity)

$$W=(\xi+f)-\frac{1}{\rho}\frac{\partial h}{\partial z} \tag{5.1b}$$

can be used as an conservative dynamic cloud property. Thus, the relationships derived in Section 4 hold for $I=(h,S_w,x,W)$ so that we are able to calculate the large-scale sources of latent and sensible heat and vorticity.

For simplicity we assume a constant vertical gradient Γ_I for the environmental distribution of the conserved quantities which is realistic in the lower troposphere. Table 2 shows the boundary conditions needed to determine the large-scale sources. This information is taken from Augstein *et al.* (1973) which is representative for a large-scale unit area ($F=2.2\times10^5$ km^2). The vertical cloud ensemble mass flux M_0 and the characteristic cloud layer depth Z are derived according to the closure conditions described in Section 4. Using Table 1 for undisturbed conditions, we calculated the total number of clouds within the area F from (4.5) yielding $N_0=14\,000$ and an area cover $\sigma=A_0F^{-1}=10\%$. Eqs. (2.10)–(2.12) describe the cloud ensemble mass budget which is shown in Fig. 1. The three terms describing

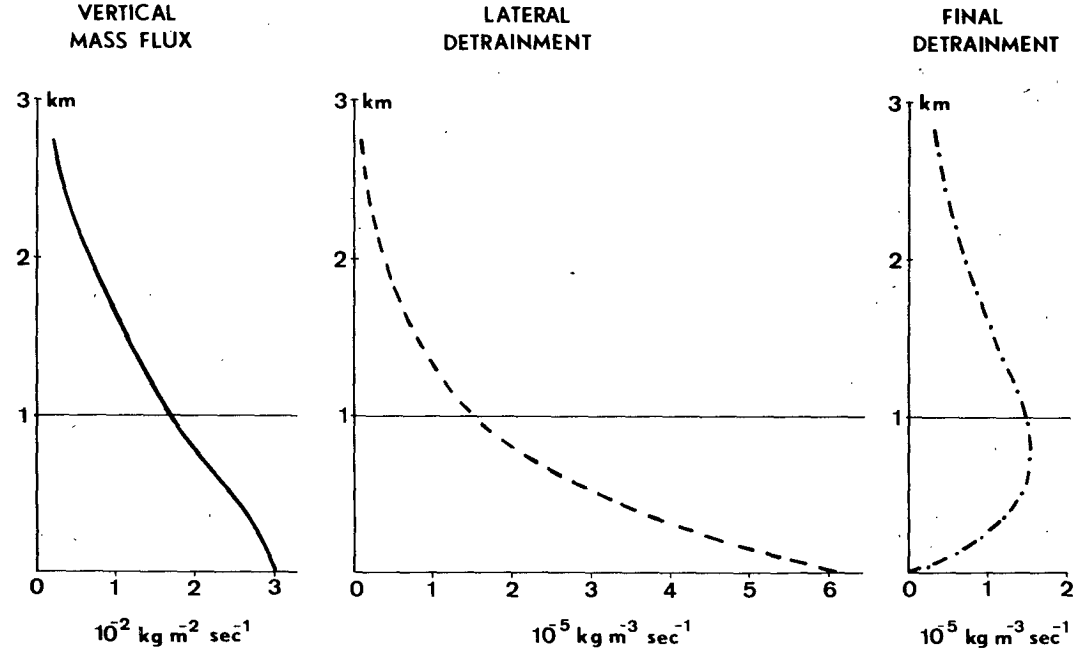

FIG. 1. Mass budget of the cloud ensemble.

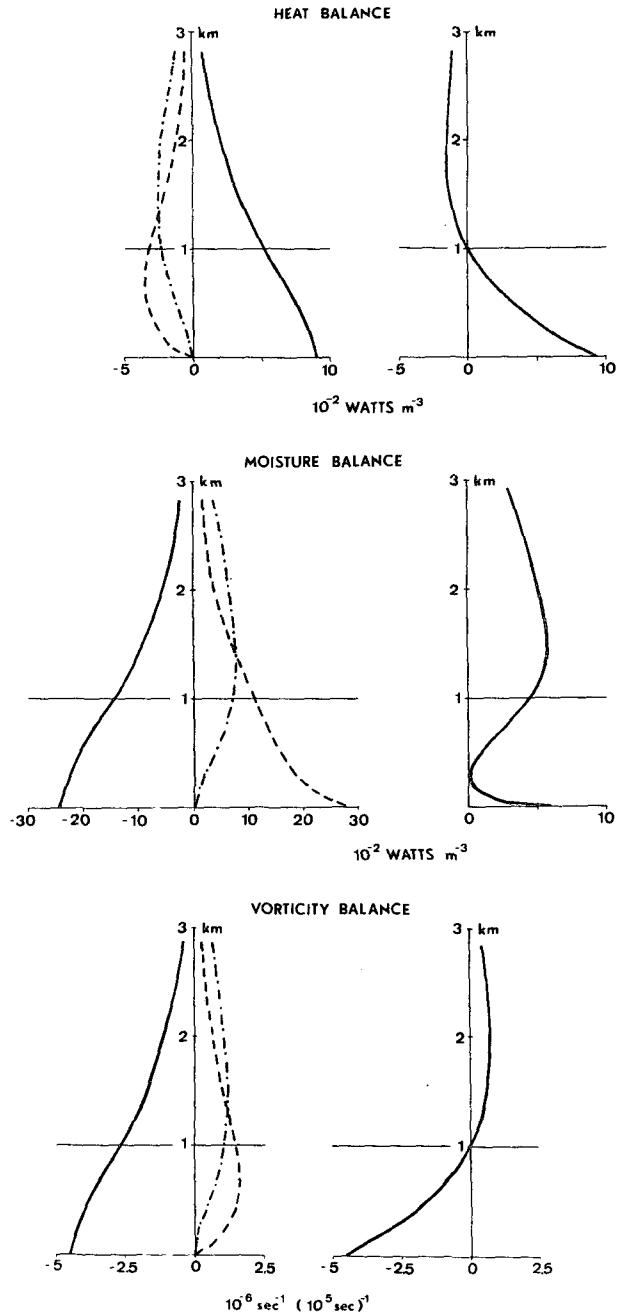

FIG. 2. Heat, moisture and vorticity budgets of the cloud ensemble. Left: compensating subsidence (full line), lateral detrainment (dashed line), final detrainment (dash-dotted line). Right: total source terms. (10^{-2} W m^{-3} ρ^{-1} can be approximated by 0.85 K day^{-1}, if the density of the cloud layer is $\rho \approx 1$ kg m^{-3}).

the large-scale sources (3.1) are specified by (3.6) and (3.7) and the mass budget equations (2.10)–(2.12); see Fig. 2.

The latent and sensible heat sources are obtained from the conserved total water content and the liquid-water static energy budgets. The liquid water and sensible heat generated by the condensation process within the cloud are carried with the rising cloud parcel. Lateral and final detrainment of these cloud properties lead to a cooling and moistening of the large-scale (environmental) field which is mainly due to the evaporation of liquid water, and slightly modified by surplus of sensible heat and specific humidity within the rising cloud parcel. Compensating subsidence, however, has a heating and drying effect on the atmosphere.

Summarizing, we find heating predominates in the lower layer, the change of sign occurring at the characteristic layer depth Z of the cloud ensemble, thus marking the inversion base. Moistening appears within the total cloud layer, the profile of which essentially depends on the environmental moisture gradient Γ_q.

The vorticity source is negative below the characteristic cloud-layer depth Z and positive above, producing anticyclonic and cyclonic vorticity, respectively. Some further comment should be made on the cloud-base boundary condition. Here, we assumed no difference of Ertel's circulation constant between cloud ensemble and environment. However, one may prefer no vorticity difference to exist which leads to the condition

$$\Delta W_0 = (W_c - \bar{W})_0 = \bar{\xi}_0 \left(\frac{\partial h_c}{\partial z}\bigg|_{z_0} - \Gamma_h \right) \rho^{-1}. \qquad (5.2)$$

Results using this relation show that the anticyclonic vorticity source is enhanced and extended beyond the characteristic cloud-layer depth Z.

The large-scale radiative heating due to the transient cloud ensemble is calculated according to the parameterizations in Section 3b and is shown in Fig. 3. For

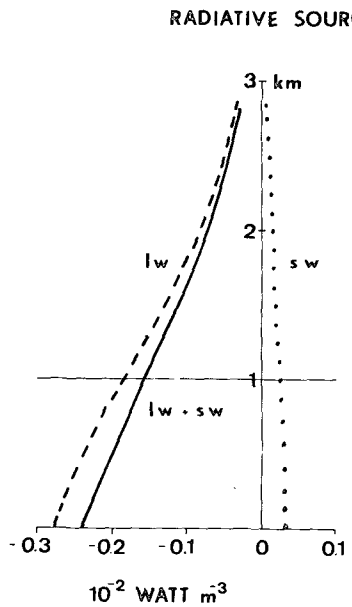

FIG. 3. Shortwave (sw) and longwave (lw) radiative heating by an ensemble of cumulus clouds.

the shortwave global radiative flux density $G=800$ W m^{-2} has been used. The magnitudes of the heating rates depend essentially on the coefficients ϵ_k and ϵ_l, whereas the profiles are determined by the vertically decreasing water content of the cloud ensemble (for shortwave absorption) and the vertical temperature distribution of the cloud tops (for longwave emission). The heating due to shortwave absorption decreases from its value at cloud base to 80% at the characteristic cloud-layer depth (inversion top) and to 15% at 3 km above cloud base, showing a more uniform distribution in the vertical than the longwave emission the related values of which are 65 and 15%, respectively. The physical mechanisms by which the effects of radiative processes in the clouds are transferred into the environment are the lateral and final detrainment processes.

With the constants used the net radiative heating amounts to about 10% of the net sensible heat source. However it should be emphasized that these magnitudes are quite sensitive to changes in the constants of proportionality ϵ_k, ϵ_l.

The above results have been compared with other budget studies using parametric schemes (e.g., Nitta, 1975) and show good agreement. However, it should be kept in mind that constant gradients have been used here to describe the vertical distribution of the conserved quantities. Although a realistic distribution improves the results, this paper was concerned solely with different aspects of cumulus parameterization by a transient cloud ensemble.

6. Conclusion

The transient cumulus cloud ensemble and the related parameterization scheme (closure condition, large-scale sources) discussed here are somewhat different from presently existing models.

1) The *cloud elements* used undergo a life cycle (in an integrated sense). They have no exponentially increasing mass flux. Furthermore, lateral detrainment processes are included as well as final detrainment at the top.

2) The *cloud ensemble* is represented by a simple statistical distribution function for the individual cloud elements, the parameters of which are prescribed by and change according to the closure condition, but not the distribution function itself. Thus, the statistical behavior of the cloud elements within the ensemble is similar and independent of the large-scale situation.

3) The *closure condition* incorporates that part of the large-scale processes providing the (entropy) flow on which the internal (dissipative) cloud structure changes (precipitating vs nonprecipitating) depend. The magnitude of this structure-changing flow determines the statistical parameters of the cloud population, i.e., cloud-base mass flux and characteristic cloud-layer depth.

4) Finally, *directly observable information* of cloud population parameters (cloud number and area cover) can be extracted from the parametric scheme. In addition, these observations can be incorporated as input parameters for the model.

It should be mentioned that this scheme (including the closure condition) is based only on geometrical and statistical properties of clouds, the structural changes of which are included. However it appears necessary to verify theoretically the statistical distribution functions describing the cloud ensemble and the qualitative arguments leading to the closure conditions. Modern theoretical thermodynamics provide sufficient tools to confirm or deny such a verification.

Acknowledgments. The author is indebted to Dr. W. Schubert and another referee for their helpful comments, Dr. H. Grassl for his advice on radiative processes, and to Ms. M. Lungwitz and U. Eckertz-Popp for preparing the manuscript.

APPENDIX

List of symbols

t, z, r	time, height above cloud base, cloud radius
ρ, w, u	density; vertical and horizontal velocity
a, A	area; individual cloud, cloud ensemble
m, M	vertical mass flux; individual cloud, cloud ensemble
d, D	mass detrainment; individual cloud, cloud ensemble
$n; K, \beta$	cloud number density, related coefficients
N	accumulated cloud number
$\lambda^*, 3\alpha$	entrainment factor, related coefficient $(3\alpha \approx 0.2)$
$Z, \hat{Z}$	characteristic cloud-layer depth, average cloud depth
τ	half-lifetime of cloud element
σ, F	fractional cloud cover, large-scale unit area
I	area averaged conserved cloud property
h, s_w	moist static energy, liquid water static energy
W	Ertel's circulation constant
x, l, q	specific total water content, liquid water, humidity
Q_I	large-scale source of I
Γ_I	vertical gradient of large-scale variable I
Δ	difference between cloud ensemble and large-scale environment
γ, c	geometrical cloud structure parameters
k, K	shortwave absorption (heating rate) of individual cloud, cloud ensemble
e, E	longwave emission (cooling rate) of individual cloud, cloud ensemble
G	global radiative flux density
ϵ_e, ϵ_k	empirical constants of proportionality

INDICES

0, t	cloud base, cloud top
c	transient cloud
l, f	referring to lateral and final detrainment
1, 2	disturbed, undisturbed large scale situation
$(-)$	large-scale average
$(\sim)$	average over growing period τ.

REFERENCES

Augstein, E., H. Riehl, F. Ostapoff and V. Wagner, 1973: Mass and energy transports in an undisturbed Atlantic trade wind flow. *Mon. Wea. Rev.*, **101**, 101–111.

Betts, A. K., 1975: Parametric interpretation of trade-wind cumulus budget studies. *J. Atmos. Sci.*, **32**, 1934–1945.

Cho, H. R., 1976: Effects of cumulus cloud activity on large scale moisture distribution as observed on Reed-Recker's composite easterly waves. *J. Atmos. Sci.*, **33**, 1117–1119.

Fraedrich, K., 1976: A mass budget of an ensemble of transitent cumulus clouds determined from direct cloud observations. *J. Atmos. Sci.*, **33**, 262–268.

Kuo, H. L., 1974: Further studies of the parameterization of the influence of cumulus convection on large-scale flow. *J. Atmos. Sci.*, **31**, 1232–1240

Nitta, T., 1975: Observational determination of cloud mass flux distributions. *J. Atmos. Sci.*, **32**, 73–91.